

A comparison of simulated and measured lake ice thickness using a Shallow Water Ice Profiler

Laura C. Brown* and Claude R. Duguay

Interdisciplinary Centre on Climate Change and Department of Geography & Environmental Management, University of Waterloo, Waterloo ON N2L 3G1, Canada

Abstract:

In northern regions where observational data is sparse, lake ice models are ideal tools as they can provide valuable information on ice cover regimes. The Canadian Lake Ice Model was used to simulate ice cover for a lake near Churchill, Manitoba, Canada throughout the 2008/2009 and 2009/2010 ice covered seasons. To validate and improve the model results, *in situ* measurements of the ice cover through both seasons were obtained using an upward-looking sonar device Shallow Water Ice Profiler (SWIP) installed on the bottom of the lake. The SWIP identified the ice-on/off dates as well as collected ice thickness measurements. In addition, a digital camera was installed on shore to capture images of the ice cover through the seasons and field measurements were obtained of snow depth on the ice, and both the thickness of snow ice (if present) and total ice cover. Altering the amounts of snow cover on the ice surface to represent potential snow redistribution affected simulated freeze-up dates by a maximum of 22 days and break-up dates by a maximum of 12 days, highlighting the importance of accurately representing the snowpack for lake ice modelling. The late season ice thickness tended to be under estimated by the simulations with break-up occurring too early, however, the evolution of the ice cover was simulated to fall between the range of the full snow and no snow scenario, with the thickness being dependant on the amount of snow cover on the ice surface. Copyright © 2011 John Wiley & Sons, Ltd.

KEY WORDS Shallow Water Ice Profiler; lake ice modelling; ice thickness; Hudson Bay Lowlands

Received 27 August 2010; Accepted 4 March 2011

INTRODUCTION

Lakes comprise a large portion of the surface cover in the northern boreal and tundra areas of Northern Canada forming an important part of the cryosphere, with the ice cover both playing a role in and responding to climate variability. The presence (or absence) of ice cover on lakes during the winter months is known to have an effect on both regional climate and weather events (e.g. thermal moderation and lake-effect snow) (Rouse *et al.*, 2008). Lake ice has also been shown to respond to climate variability; particularly changes in air temperature and snow accumulation. Both long- and short-term trends have been identified in ice phenology records and are typically associated with variations in air temperatures; while trends in ice thickness tend to be associated more with changes in snow cover (Brown and Duguay, 2010).

During the ice growth season, the dominant factors that affect lake ice are temperature and precipitation. However, once the ice has formed, snow accumulation on the ice surface then slows the growth of ice below due to the insulating properties as a result of the lower thermal conductivity (thermal conductivity of snow, $0.08\text{--}0.54\text{ Wm}^{-1}\text{ K}^{-1}$ vs $2.24\text{ Wm}^{-1}\text{ K}^{-1}$ for ice, (Sturm *et al.*, 1997)). Snow mass can change the composition of the ice

by promoting snow ice development, and hence influence the thickness of the ice cover (Brown and Duguay, 2010).

In northern regions where observational data is sparse, lake ice models are ideal for studying ice cover regimes as they can provide valuable information including timing of break-up/freeze-up, ice thickness and composition. Several different types of models have been used to investigate the response of lake ice to external forcing(s), with varying degrees of complexity such as regression or empirical models (Palecki and Barry, 1986; Livingstone and Adrian, 2009), energy balance models (Heron and Woo, 1994; Liston and Hall, 1995) and thermodynamic lake ice models (Vavrus *et al.*, 1996; Launiainen and Cheng, 1998; Duguay *et al.*, 2003). Application of these models has been effective in examining the effects of altering the air temperatures and snow depths on lake ice thickness by sensitivity analysis (Vavrus *et al.*, 1996, Ménard *et al.*, 2002, Morris *et al.*, 2005). Overall, changes in snow depths had more of an impact on ice thickness than changes to air temperatures. Decreasing the amount of snow cover tended to result in thicker ice formation (Brown and Duguay, 2010). However, snow with higher snow water equivalent accumulating on the ice surface can also lead to an increase in ice thickness as a result of increased snow ice formation (Korhonen, 2006).

Modelling provides an opportunity to further understand the interactions between lake ice and climate, which is important for examining potential changes in northern

*Correspondence to: Laura C. Brown, Interdisciplinary Centre on Climate Change and Department of Geography & Environmental Management, University of Waterloo, Waterloo ON N2L 3G1, Canada.
E-mail: lcbrown@uwaterloo.ca

ice regimes under future anticipated changes in the climate system. However, before future conditions can be explored, models need to be validated against current conditions to improve predictions. Validation of modelled ice thickness in northern Canada presents unique difficulties as frequent sampling is not logistically feasible in remote locations and ice thickness on small lakes is not easily obtainable from remote sensing imagery. A useful tool for validation of the ice thickness is the Shallow Water Ice Profiler (SWIP) manufactured by ASL Environmental Sciences Inc. This upward-looking sonar device was developed for shallow water studies based from the well-established ice profiling sonar (IPS) that has been used for more than a decade to examine sea ice drafts in the polar and sub polar oceans (Melling *et al.*, 1995; Jasek *et al.*, 2005; Marko and Fissel, 2006). The SWIP has primarily been used to study river ice drafts to date (Jasek *et al.*, 2005; Marko *et al.*, 2006) and this study represents the first application of an SWIP for comparing measured ice thickness to model simulations in a shallow lake.

The objective of this study is to examine the effectiveness of the Canadian Lake Ice Model (CLIMo) at simulating ice thickness compared to *in situ* ice thickness measurements using an upward-looking IPS, complemented by traditional manual measurements and digital camera imagery.

STUDY AREA AND METHODOLOGY

The selected lake for this study, Malcolm Ramsay Lake (previously known as Lake 58), is situated within the Hudson Bay Lowlands in a forest-tundra transition zone near Churchill, Manitoba (58.72°N, 93.78°W) (Figure 1). The lake covers an area of 2 km² with a mean depth of 2.4 m (maximum depth of 3.2 m) (Duguay *et al.*, 2003). The mean annual temperature in Churchill

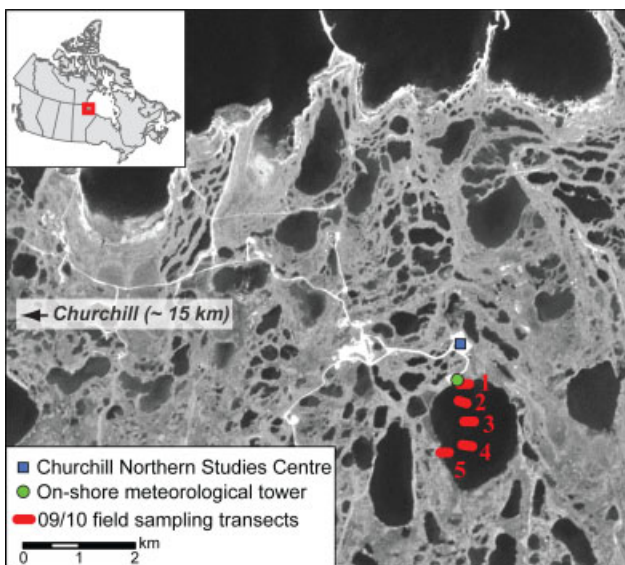


Figure 1. Location of Malcolm Ramsay Lake, near Churchill, Manitoba. Sampling transects shown with identifying numbers

is -6.9°C with only June to September temperatures reaching above 0°C . Total precipitation is 432 mm, with an annual snowfall of 191 cm.

The model used is the CLIMo, a one-dimensional thermodynamic model used for freshwater ice cover studies (Ménard *et al.*, 2002; Duguay *et al.*, 2003; Jeffries *et al.*, 2005, Morris *et al.*, 2005) capable of simulating ice on and off, thickness and composition of the ice cover (clear or snow ice). CLIMo has been modified from the 1-D sea ice model of Flato and Brown (1996), which was based on the 1-D unsteady heat conduction equation, with penetrating solar radiation, of Maykut and Untersteiner (1971), i.e.

$$\rho C_p \frac{\partial T}{\partial t} = \frac{\partial}{\partial z} k \frac{\partial T}{\partial z} + F_{sw} I_0 (1 - \alpha) K e^{-Kz} \quad (1)$$

where ρ (kg m^{-3}) is the density, C_p ($\text{J kg}^{-1} \text{K}^{-1}$) the specific heat capacity, T (K) the temperature, t (s) the time, k ($\text{Wm}^{-1} \text{K}^{-1}$) the thermal conductivity, z (m) the vertical coordinate, positive downward, F_{sw} (Wm^{-2}) the downwelling shortwave radiative energy flux, I_0 the fraction of shortwave radiation flux that penetrates the surface (a fixed value dependent on snow depth), α the surface albedo and K the bulk extinction coefficient for penetrating shortwave radiation (m^{-1}).

The surface energy budget can then be calculated:

$$F_o = F_{lw} - \varepsilon \sigma T^4(0, t) + (1 - \alpha)(1 - I_0)F_{sw} + F_{lat} + F_{sens} \quad (2)$$

where F_o (Wm^{-2}) is the net downward heat flux absorbed at the surface, ε the surface emissivity, σ the Stefan-Boltzmann constant ($5.67 \times 10^{-8} \text{ Wm}^{-2} \text{K}^{-4}$), F_{lw} (Wm^{-2}) the downwelling longwave radiative energy flux, F_{lat} (Wm^{-2}) and F_{sens} (Wm^{-2}) the latent heat flux and sensible heat flux, respectively (both positive downward) (Ménard *et al.*, 2002; Jeffries *et al.*, 2005).

CLIMo includes a fixed-depth mixed layer in order to represent an annual cycle. When ice is present, the mixed layer is fixed at the freezing point and when ice is absent, the mixed layer temperature is computed from the surface energy budget and hence represents a measure of the heat storage in the lake. The water column of shallow lakes is typically well-mixed and isothermal from top to bottom during the ice-free period, permitting the mixed layer depth to be a good approximation of the effect of lake depth leading to autumn freeze-up (Duguay *et al.*, 2003).

Melt at the upper surface of the ice is determined by the difference between the conductive flux and the net surface flux; the snow (if any) on the ice surface is melted first and the remaining heat is used to melt the ice. The growth and melt of the ice cover at the underside is determined by the difference between the conductive heat flux into the ice and the heat flux out of the upper surface of the mixed layer. The shortwave radiation that penetrates through the bottom of the ice cover is assumed to be absorbed by the mixed layer and returned to the ice underside in order to keep the temperature of the mixed layer at the freezing

point (Duguay *et al.*, 2003). The current version of the model includes a simplified heat exchange between the water column and the lake sediments in the form of a constant heat flux, rather than a varying heat flux that fully captures the annual cycle; this is an area that will be addressed in a future version of the model.

Snow ice is created by the model if there is a sufficient amount of snow to depress the ice surface below the water level. The added mass of the water filled snow pores (slush) is added to the ice thickness as snow ice. The amount of snow ice formed (if any) is not taken into account when melting the ice slab. The albedo parameterization in CLIMo is based mainly on surface type (ice, snow or open water), surface temperatures (melting *vs* frozen) and ice thickness, with no distinction regarding ice composition. A more detailed description of CLIMo can be found in Duguay *et al.* (2003).

The model was driven by daily on-shore meteorological data from an Automated Weather Station (AWS) using Campbell Scientific equipment. Input data for the model included air temperature and relative humidity (HC-SC-XT temperature and relative humidity probe), wind speed (RM Young Wind Monitor), and snow depth (SR50A Sonic Ranging Sensor). In addition to the AWS data, cloud cover data was obtained from the Meteorological Service of Canada's Churchill weather station, located approximately 16 km to the west. A modification to CLIMo was made for this study to incorporate measured incoming solar radiation at the AWS (CNR-1 Net Radiometer) rather than the model's internal calculations for solar radiation based on latitude and cloud cover. A second modification to CLIMo was made wherein measured snow density values from on-ice measurements (ranging from 171.1 kgm⁻³ to 364.3 kgm⁻³ over the season) were used rather than a fixed value for cold and warm snow. All model simulations used the weekly snow measurements made on ice during the 2009/2010 season. A Campbell Scientific digital camera (CC640 Digital Camera) was installed on the AWS, capturing hourly images of the lake to allow for on-site observations of the ice processes. To account for snow redistribution across the lake ice surface, the ice cover for two seasons (2008/2009 and 2009/2010) was simulated using a series of snow cover scenarios (0, 5, 10, 25, 50 and 100% of the on-shore snow cover depths).

To validate and improve the model results, *in situ* measurements of the ice cover formation and decay were obtained using a SWIP—an upward-looking sonar device installed on the bottom of the lake within the field of view of the digital camera. The SWIP consists of a 546 kHz acoustic transducer, pressure transducer, thermometer, two axis tilt sensors and a battery pack capable of long deployments (Figure 2). The SWIP was programmed for target detection, collecting target data (scanning the water column for acoustic backscatter returns from a target, e.g. ice, water–air interface) every 1 s (10 s from January to March) and measuring instrument temperature, pressure and tilt data every 60 s. On-shore barometric pressure at the AWS (61 205V Barometric Pressure Sensor) was

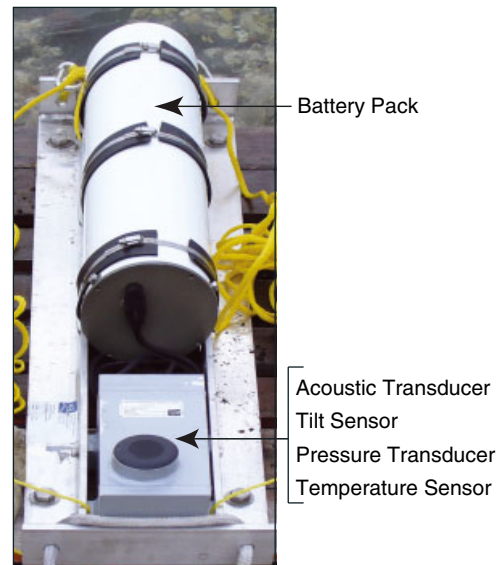


Figure 2. Shallow Water Ice Profiler

used in combination with the pressure transducer on-board the SWIP to determine local water levels over the seasons. The acoustic ranges to the bottom of the ice cover measured by the SWIP were corrected for the instrument tilt, variations to the speed of sound in water (based on temperature) and subtracted from the local water levels to determine the thickness of the ice (Melling *et al.*, 1995; Marko and Fissel, 2006).

During the spring of 2009 (13 April to 27 June), weekly measurements of on-ice snow depth, thickness of the snow ice layer (if present) and total ice thickness were obtained (approximately four samples averaged for each per sampling date). Throughout the ice covered season of 2009/2010 (15 November 2009 to 6 April 2010) five transects were used for sampling (Figure 1), weekly measurements were taken of on-ice snow depth (100 depth samples from each of the five transects); on-ice snow density (ten samples for each of the five transects); thickness of the snow ice layer (if present) and total ice cover thickness (five samples for each of the five transects). The sampling transect closest to the location of the SWIP was used for comparison between the SWIP, simulated ice thickness and on-shore snow depths.

One challenge in comparing simulations to observations of ice cover is the differing definitions used. Freeze-up and break-up are observable processes occurring over time and space, while the SWIP data is at a single point in the lake and the simulated freeze-up and break-up dates from the model are an instantaneous, 1-D, event based on ice thickness (Jeffries *et al.*, 2005). To minimize discrepancies in terminology, the date at which the simulations formed a permanent cover for the season is referred to as complete freeze over, while the first day of open water simulated is referred to as water clear of ice. The SWIP freeze-up and break-up dates are defined as the first date when ice/open water is detected above the sensor. The camera imagery is more subjective, and freeze-up is defined as the time between first visible ice

in the camera view (freeze-onset) until a solid ice cover is formed (complete freeze over). Surface ice decay is defined as the time from when a portion of ice is visibly beginning to melt (snow free, wet/slushy surface) and break-up is defined as the date from the first appearance of open water until the water is free of ice (water clear of ice). The ice season referred to throughout the article is defined as the time from ice formation in the autumn to water clear of ice in the following summer.

RESULTS AND DISCUSSION

Field measurements and observations of the ice cover

2008/2009 Season. Ice formation was periodically visible in the camera imagery starting on 20 October and formed a solid cover by 27 October. The SWIP detected the ice formation on 26 October (Figures 3(a) and 4). The ice thickened throughout the season until 22 March 2009 (143 cm) at which point it exceeded the lower limit of the detection ranges programmed into the SWIP. However, field measurements provided the ice thicknesses during the time the SWIP was unable to record the lower levels of the ice cover (maximum ice thickness sampled was 165 cm on 5 June). Visible ponding, shushing and surface melt were seen in the camera imagery from ~11 June to 9 July, with the first open water visible on 26 June (Figure 3(c)). Field measurements of on-ice snow thickness showed the absence of snow cover on the lake ice by 11 June, with the SWIP detecting water levels rising after this date. An interesting event was noted in

the SWIP readings during the ice cover decay. The tilt data from the sensor showed it being slowly tilted on both on the vertical and horizontal axes for a number of days beginning on 14 June, tilting as far as 20° on the horizontal axis before returning to a steady near level by 27 June. This event is likely attributed to the ropes that were attached to the back-end of the SWIP frame for retrieval purposes being frozen into the ice, pulling the sensor and frame upwards as the ice cover rose with the influx of snowmelt before melting/breaking free of the ice draft. The SWIP detected open water by 7 July, resulting in an ice cover duration for the 2008/2009 season of 252 days. While the camera images also show open water in the approximate location of the SWIP on this date, floating ice continues to drift through the camera field of view until 9 July (Figure 3(d)).

2009/2010 Season. During the 2009/2010 ice cover season, ice formation was detected by the SWIP on 14 October and seen from the camera imagery on 13 October, with a solid cover formed by 15 October. Snow began accumulating on the ice surface by early November, with brief snow cover on 20–22 October. Thickening of the ice cover occurred until the maximum depth was reached on 15 April (98 cm) based on the SWIP and measured manually at 94 cm (as of 29 March at the sampling location nearest the SWIP). The camera imagery showed a section of the ice to be snow free on 10 May, snow covered again from 21 to 30 May, visibly melting from 31 May and open water appearing

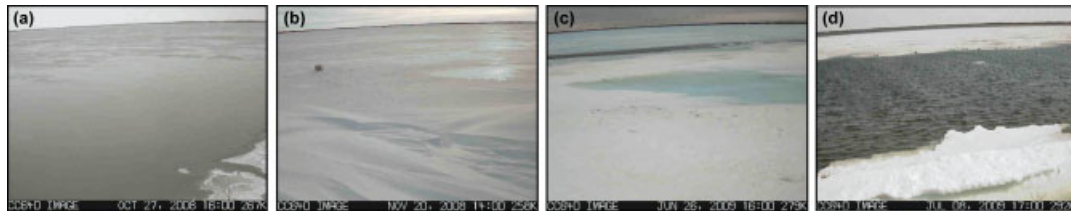


Figure 3. (a) Ice cover formation (27 October 2008), (b) snow redistribution on the ice surface (20 November 2008), (c) ice break-up in progress with open water and slush visible on the ice surface (26 June 2009) and (d) redistribution of floating ice pans just before the end of break-up (8 July 2009)

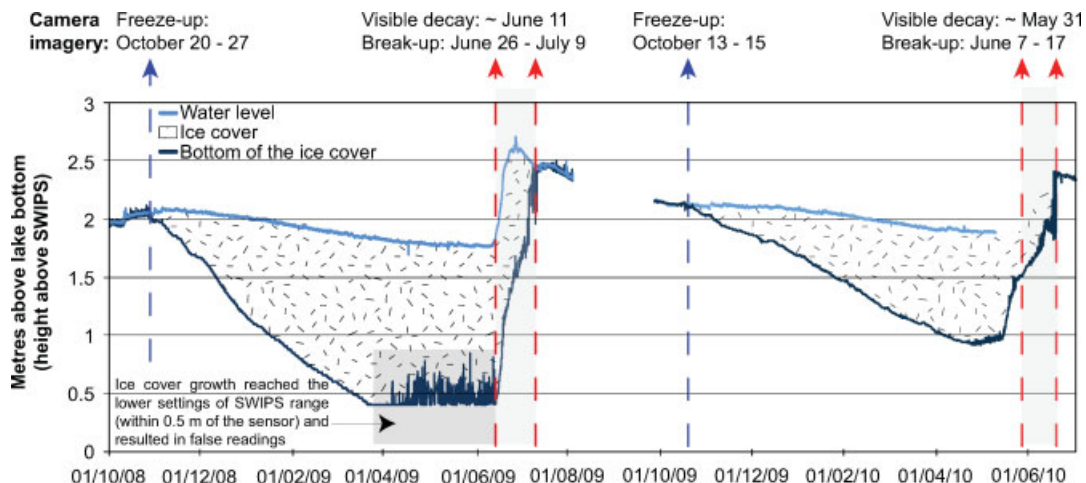


Figure 4. Water level and ice cover ranges measured by the SWIP. Coinciding dates of events observed from the digital camera noted above graph

Table I. Comparison of monthly average air temperatures (°C) between the two ice seasons

	October	November	December	January	February	March	April	May	June	July
2008/2009	1.09	-8.48	-26.11	-23.21	-23.02	-21.42	-8.17	-6.65	2.46	7.93
2009/2010	-0.46	-6.57	-20.59	-21.27	-19.52	-10.04	-3.48	-1.81	6.97	13.88

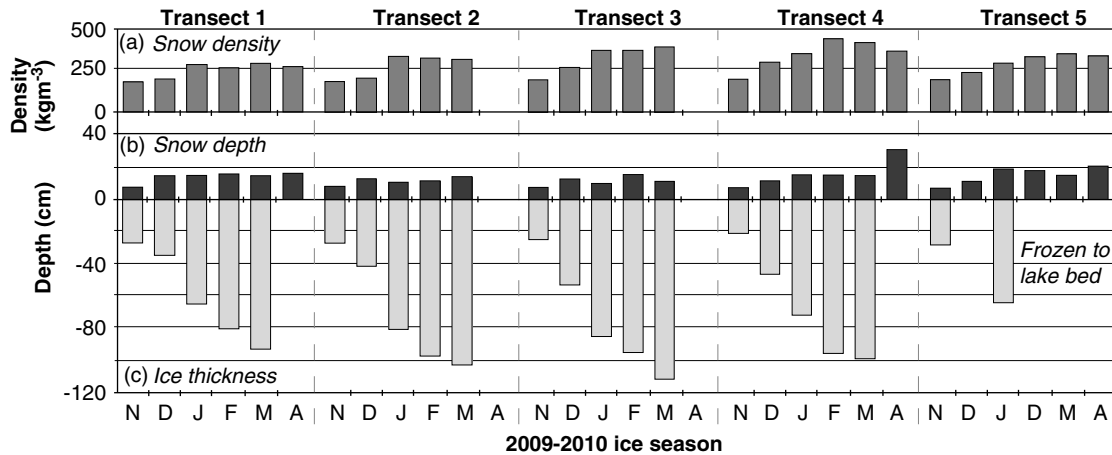


Figure 5. (a) Monthly average density (kg m^{-3}), (b) snow depth (cm) and (c) ice thickness (cm) from sampling transects on the lake ice surface 2009/2010. Location of the transects shown in Figure 1

by 7 June. Water levels from the SWIP were not available during the melt season due to a power supply issue, which prevented the calculation of the ice thickness after May. Both the SWIP and the camera imagery detected open water on 13 June, followed by moving ice floes on 14 June, and returning to open water by 15 June (with the exception of near shore ice seen in the imagery, which was fully melted by 17 June). The 2009/2010 ice season was on average 4°C warmer than 2008/2009 season (Table I). This resulted in a thinner ice cover forming, allowing for a complete season of ice readings from the SWIP, with an ice cover duration of 243 days.

Snow cover variability on the lake ice surface

Snow cover is known to be an important determinant for lake ice thickness. Snow redistribution by wind and associated changes in depth and density of the snow pack contribute to variations in ice thickness (Brown and Duguay, 2010). Weekly snow depth and density measurements during the 2009/2010 season highlight the variability present in the snow cover across the lake surface both spatially and temporally (Figure 5). The snow density and depth measurements fluctuate throughout the season differently at each of the transects (for locations, Figure 1), with the most variability found at one of the central lake locations (Transect 4). Seasonal average density increases with distance from shore for Transects 1 through 3, with the highest densities found at Transect 4; while Transect 5, which was situated along a shallower shoreline, had densities in the mid-range of the others. Expectedly, snow depth tended to be slightly higher towards the shore overall (Adams and Roulet, 1984), however, the highest snow depths measured were from a central lake transect (Transect

4) on 6 April (30 cm), a 12.1 cm increase from the previous measurement. An increase of only 5 cm was measured on the same date at the near-shore transect (Transect 5), while on-shore snow accumulation during this time was 18 cm during the snowfall events on 5 and 6 April—again highlighting the variability present in the snow cover across the lake. The thickest ice was measured in March at Transect 3 (111 cm); however, no April measurements were available.

A monthly summary of the 2009/2010 snow measurements and ice thickness can be found in Table II. Snow depth had little variation from December to March, with spring snowfalls increasing the depth (no on-ice measurements from May were available). Snow density increases throughout the season, with the exception of the April measurements, which consisted of only one date. Comparing the snow depths measured at Transect 1 (the nearest transect to the location of the SWIP) to the snow depths on shore at the AWS shows a ratio of 25% snow-on-ice to show-on-shore (Figure 6). Seasonal variations are noted in early 2009 with a ratio of 10 and 23% before and after the spring snowfall events. The large difference between the measured snow depth on the ice and at the AWS is due to a combination of redistribution by wind over the lake ice surface, and drifting and trapping of snow by the shrubs beside the AWS on shore.

Previous work by Duguay *et al.* (2003) showed through modelling that much of the variability in ice thickness and break-up dates were driven by snowfall. Several studies have examined the effects on lake ice thickness through altering snow depths; finding overall, that decreasing the amount of snow cover resulted in thicker ice formation (Vavrus *et al.*, 1996; Ménard *et al.*,

Table II. Monthly average of the mean and standard deviation of lake-wide snow and ice measurements (2009/2010)

	Snow depth (cm)		Snow density (kg m ⁻³)		Ice thickness (cm)	
	Mean	Standard deviation	Mean	Standard deviation	Mean	Standard deviation
November	7.2	0.5	195.3	5.7	25.7	2.8
December	12.2	1.3	248.0	42.7	43.9	7.9
January	13.4	3.7	335.3	34.9	72.0	8.4
February	14.7	2.2	355.4	63.6	92.0	7.8
March	13.5	1.6	362.1	49.4	101.7	7.5
April	21.9	7.5	334.4	43.5		

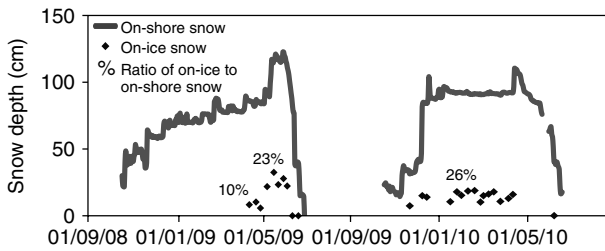


Figure 6. Comparison of the measured snow depth on shore at the AWS and on the ice from field sampling and the ratio between them

2002; Morris *et al.*, 2005). To determine the best snow-fall representation for the on-ice snow depths, several simulations were generated with varying percentages of the on-shore snow depth.

Model simulations

Ice thickness was simulated using the following snow cover scenarios: 0, 5, 10, 25, 50 and 100% of the on-shore snow depths at the AWS (Figure 7). During the first season (2008/2009), all simulations had complete freeze over on 26 October (Table III). The ice thickened throughout the season at different rates based on the snow cover scenarios. A 0–25% snow cover resulted in progressively more ice growth as snow cover decreased (with little to no snow ice formation), while 50% snow

cover resulted in slightly thicker ice cover than the 25%. The full snow scenario was similar to the 10% scenario until early April, at which point the formation of snow ice in the full snow scenario continued to increase the total thickness of the ice for the remainder of the season. While the 25–100% snow cover scenarios had fairly similar ice thickness for the first half of the ice season (<10 cm difference between them until late February) the ratio of snow ice to clear ice differed between them (progressively more snow ice formed with increase in snow cover scenario). The maximum ice thicknesses varied between the scenarios (Table IV) with the least from the 25% scenario (128 cm) and maximum from the 0% scenario (176 cm). Melt began first in the 0% snow cover, briefly in mid-April then continued in late May, at which point the rest of the scenarios began melt—resulting in a variation of 13 days between the scenarios to reach water clear of ice.

During the second season (2009/2010), the ice cover formed on 14 October for all scenarios (Table III). Ice growth followed the same pattern as the 2008/2009 season, with the thickest ice forming from the 0% snow cover scenario followed by the 5 and 10% scenarios, with the 25 and 50% scenarios forming slightly thinner or equal amounts as the 100% snow cover scenario. After two substantial snowfalls in December, the remaining

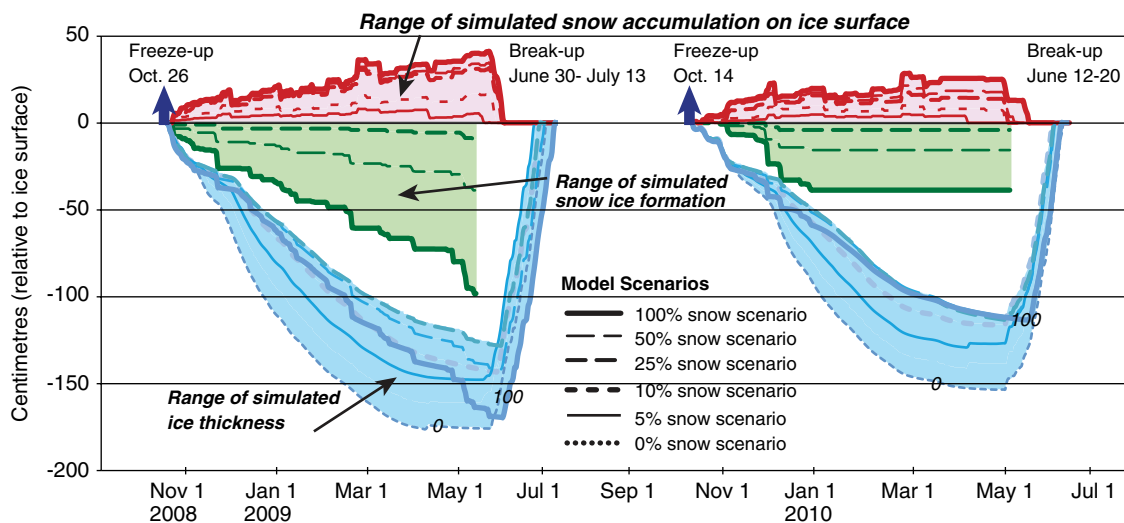


Figure 7. Model simulations of snow on ice, depths of snow ice and total ice thickness for each snow cover scenario (0, 5, 10, 25, 50 and 100% accumulation) to represent potential snow redistribution on the ice surface. Melt is not shown for the simulated snow ice as CLIMo does not distinguish between ice compositions during melt

Table III. Complete freeze over, water clear of ice and ice cover duration simulated by CLIMo for various snow cover scenarios

Snow cover scenario (%)	2008–2009 Complete freeze over (2008)	Water clear of ice (2009)	Ice cover duration (days)	2009–2010 Complete freeze over (2009)	Water clear of ice (2010)	Ice cover duration (days)
100	26 October	13 July	260	14 October	18 June	248
50	26 October	7 July	254	14 October	14 June	244
25	26 October	3 July	250	14 October	13 June	243
10	26 October	3 July	250	14 October	12 June	242
5	26 October	30 June	247	14 October	13 June	243
0	26 October	9 July	256	14 October	20 June	250

Table IV. Maximum ice thickness simulated by CLIMo for various snow cover scenario simulations

Snow cover scenario (%)	2008–2009 Maximum ice thickness (cm)	Date	2009–2010 Maximum ice thickness (cm)	Date
100	170	8 June	114	26 May
50	142	7 June	112	12 May
25	128	6 June	114	11 May
10	143	3 June	116	5 May
5	148	23 May	127	3 May
0	176	1 June	154	6 May

snow accumulation during 2010 recorded by the on-shore snow sensor increased gradually (rarely more than 1 cm at a time). While snow did continue to accumulate, the weight of the additional snow was not enough to depress the ice to cause slushing and form any addition snow ice. This resulted in the 2009/2010 season having less than half as much snow ice as 2008/2009 for the 100% snow cover scenario (39 vs 103 cm). With little accumulation in the early 2010 months, the differences between the snow cover scenarios were small, resulting in similar ice thicknesses for the 25–100% snow cover scenarios, albeit with different ratios of snow ice to clear ice. These similar scenarios diverged during the melt season due to the differing amounts of snow on the surface that was required to melt. Maximum ice thickness did not vary as much for the 2009/2010 season with 0% snow cover scenario reaching 154 cm, 5% scenario reaching 127 cm and the rest of the scenarios ranging between 111 and 116 cm (Table IV). The removal of the ice cover was simulated between 12 and 20 June in 2010, resulting in a variation of 8 days between simulations for water clear of ice.

Despite the differing snow covers on the ice, the 25 and 50% (2008/2009) and 25–100% (2009/2010) scenarios formed similar ice thicknesses within their respective years. The ratio of snow ice to clear ice within the scenarios is, however, different. The 100% scenario for 2008/2009, while similar to the 25 and 50% scenarios for the first half of the ice season, showed that the dominant means of ice growth from February to April was the addition of snow ice, indicated by the similar increases in ice thickness on dates when snow ice was formed. With less than 25% snow cover the conductive heat loss through the ice/snow exceeded the insulating

properties of the thinner snow pack and thicker clear ice was formed with little to no snow ice. Previous work by Ménard *et al.* (2003) found the maximum ice thickness simulated became 17 cm greater for each 25% reduction in snow cover in the Back Bay area of Great Slave Lake, NWT, Canada, while Morris *et al.* (2005) found that the reduction in the snow cover by 100% resulted in a doubling of the total ice thickness for shallow lakes in central Alaska. Reduction in the snow cover to 50% of full snow for the Alaskan lakes resulted in slightly thinner ice as was also observed in this study. Reduction in the snow to 25% of the full snow scenario for the Alaskan lakes resulted in slightly larger maximum ice thickness than the full snow scenario, while this study showed slightly thinner or the same ice thicknesses from the 25 and 100% snow scenarios (with the exception of the increase as a result of snow ice in 2008/2009). This pattern of reducing snow cover resulting in thinner ice to a certain threshold was also identified by Vavrus *et al.* (1996) for Lake Mendota (Wisconsin), where decreasing snow simulations resulted in break-up dates earlier for the 75 and 50% snow scenarios because of the reduction in insulating properties of the snow, but became delayed again for 25% and the no snow scenario as a result of the increasing conductive heat loss from the ice surface. By contrast, simulations for Barrow, Alaska (Duguay *et al.*, 2003) show continuing increase in ice thickness with decreasing snow cover—however, the differing snow cover conditions between Barrow and Churchill (mean density used for simulations in Barrow was 350 kgm^{-3} vs 276 kgm^{-3} mean density for Churchill in this study) and lack of snow ice formed in Barrow are the expected reasons for the difference.

Observed versus simulated ice covers

2008/2009. All the snow cover scenarios simulated the initial ice thickening well until mid-November, at which point the simulations diverge, with the 10–100% snow cover scenarios thickening more gradually than the measured ice thickness (Figure 8). After this divergence, the 5% snow cover scenario most closely matched the measured ice thickness. This shift in the ice thickness regime is likely related to the substantial redistribution of the initial snow cover that occurred just before 20 November (Figure 3(b)). While the 5% snow cover scenario simulated the measured SWIP data through the winter to the loss of the SWIP's record (end of March),

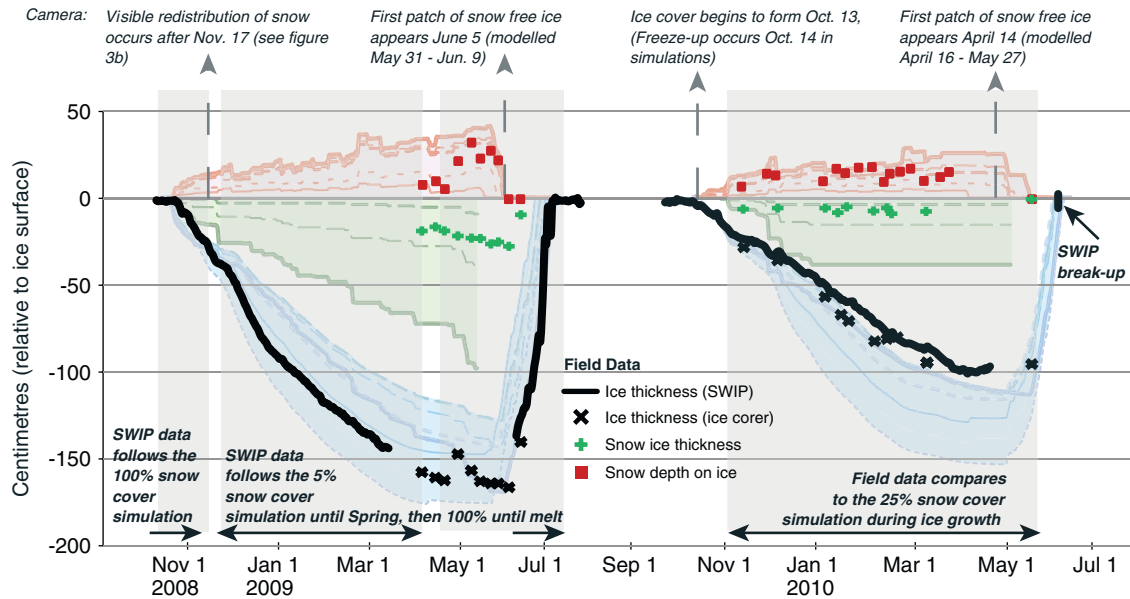


Figure 8. SWIP ice thickness data and field measurements of ice thickness, type and snow depth, superimposed on Figure 7

field measurements indicate the ice to be thicker than that produced by the 5% simulation. Throughout May, several snowfall events occurred which increased the snow depth on the ice beyond that simulated in the 5% snow cover scenario (Figures 7 and 8), with depths on ice closer to those from the 25% snow cover simulation. Virtually, no snow ice was generated by the 5% and 10% snow scenarios (~ 1 cm), however, nearly 30 cm was measured at the onset of melt (~ 10 June), which falls between the 25 and 50% snow cover simulations. Slushing caused by the additional weight of the snow in the spring resulted in an increase in snow ice that was not captured by the reduced snow cover simulations. The full snow scenario did capture the continued formation of snow ice through the spring, resulting in the 100% scenario reaching the maximum depth of the field measurements just before melt—albeit with three times more snow ice simulated than measured. With less ice thickening in the spring, the reduced snow cover scenarios under-represented the total ice thickness.

Snow melt on the ice surface was simulated well for the 25–100% snow covers (within 2 days of observations), however, even though the 25 and 50% simulations under-represented the ice thickness, break-up occurred within 3 days of observations for those scenarios. As well, since the 0–10% snow cover scenarios did not correctly represent the amount of snow on the ice in the spring, they became snow free too early and hence began ice melt too early. The full snow scenario shows similar melt to the SWIP measurements until just before the observed water clear of ice, at which point the measurements show the remaining 50 cm of ice cover to decay fully in 2 days, while the full snow scenario ice cover persists a further 6 days. This is likely due to the 1-D aspect of the model not capturing any lateral heat inputs from the open water visible in the camera imagery, which would have accelerated the final decay. The discrepancy between the

pre-melt thicknesses of the reduced snow cover scenarios and the measured ice thickness resulted in water clear of ice being simulated up to 7 days early, while the full snow scenario that did reach the maximum ice thickness simulated water clear of ice 6 days too late.

2009/2010. Field measurements during the 2009/2010 field season show different ice conditions than those from the last year. The first visible formation of ice was detected in the camera imagery on 13 October and by the SWIP on 14 October, which coincided with the formation of ice in the simulations (14 October). Other than trace amounts of drifting near the shore, snow cover did not begin to accumulate on the ice surface until early November, with the exception of a brief snow cover from 20 to 22 October. The simulated ice cover thickened similarly to the SWIP measurements until early November, while field measurements (commencing on November 15) closely followed the patterns from the 25 to 100% snow cover simulations. Measurements show the on-ice snow depths to range between the 25 and 100% snow cover scenarios as well until February at which point measurements were closer to the 25% snow cover scenarios. Throughout the winter season the simulations and field measurements are quite similar, however, the SWIP measurements show the ice to be slightly thinner. This discrepancy is likely a result of local variations in the ice cover, as the field measurements were not taken directly over the SWIP in order to avoid contaminating the sensor view. An ice thickness measurement from 30 May shows the ice decay to be within the range of the simulations. Water clear of ice ranged from 12 June to 20 June in the simulations (with the 10–50% scenarios all between 12 and 14 June), compared to 7–13 June from the camera imagery and 13 June from the SWIP (excluding the pieces of floating ice on the 14 June).

Simulations from the Fairbanks, Alaska, area done by Duguay *et al.* (2003) using a constant snow density for the season found that while CLIMo simulated the total thickness well, the results underestimated the snow ice thickness and they suggested that a better account of the density changes over the season might improve upon these results. Using a variable density over the season measured on ice for this study showed the snow ice thickness simulated by CLIMo was within 1 cm of the mean measurements for the season (6 cm) based on the 25% snow cover scenario which fit the snow-on-ice and total ice thickness adequately as well. This suggests that the slushing events early in the season were well represented by the model when the on-ice snow conditions were correctly represented.

CONCLUSIONS

The SWIP is an excellent tool for monitoring lake ice growth and was able to identify areas of the model simulations that require improvements with respect to timing and thickness of the ice cover. Formation of the ice cover was well simulated for 2008/2009, and the evolution of the ice cover depended on the snow cover scenario. For 2009/2010 the 25% snow cover scenario simulated the ice thickness most suitably with respect to the SWIP and field data—as the ratio of snow-on-ice to snow-on-shore did not deviate greatly from 25% over the season. As well, changes to the overlying snow pack create changes in the ice thickness regimes within the season, e.g. the redistribution event in November 2008 changing the ice thickness from the 100 to 5% snow cover scenario, and snowfall on the ice May 2009 creating more snow ice than the reduced cover scenarios can represent. Changing the snow cover scenarios to represent the snow redistribution did not affect the simulated freeze-up dates but did affect the break-up dates by 13 and 8 days (2008/2009 and 2009/2010, respectively), highlighting the importance of snow cover on the ice.

An accurate representation of the snow conditions on the ice (depth and density) is important for attaining the correct ice thickness. Allowing the density to vary throughout the season for the simulations provided the most consistent results from the 2009/2010 season—the time span when the density measurements were made; simulations were most similar to the 25% scenario for freeze-up and break-up, snow depth on ice, snow ice and total thickness. Using those densities to represent density for other years might not be representative of the snow conditions in those years. As no field measurements were available before April 2009, the percentage of the AWS snow actually on the ice surface, and its density, are unknown. As of April 2009, 10% of the snow received at the AWS is present on the ice surface, and while that ratio may have prevailed during the winter the simulations based on the 2009/2010 densities suggest that a 5% snow cover scenario was present.

The maximum ice thickness for 2008/2009 was captured in the simulations, although one single snow cover

scenario was not able to represent the entire season. The early half of the season was similar to the 5% snow cover scenario and the latter half of the season more resembled the full snow cover scenario after the addition of the snow ice in the spring. The simulations for 2009/2010, however, were able to capture the ice evolution fairly well throughout the season with the 25% snow cover scenario. The ice formed from the 25% snow cover scenario in 2009/2010 was too thin compared to the one available field measurement during the melt season suggesting that melt may be occurring too quickly in the early stages of decay. The current method for albedo parameterization in CLIMo does not take snow ice into account during melt. The higher albedo from the more reflective snow ice would slow the melt rate of the ice compared to an ice cover composed of purely clear ice with a lower albedo, so the observed melt rate at this point in the season is likely slower than that from the simulations. As seen in 2008/2009, the observed ice decay from the SWIP shows accelerated melt in the final days before water clear of ice compared to the simulations, this would likely have occurred in 2009/2010 as well (based on similar melt patterns on the lake from the camera imagery) and may have compensated for the early melt—resulting in break-up simulated correctly with the 25% snow cover scenario even though the melt rates may not have been captured correctly.

This suggests two separate areas of the model need to be addressed: the ratio of snow ice formation to clear ice and the albedo parameter during melt. Measurements collected on the ice surface (e.g. snow depth, snow density and snow/ice albedo) would be particularly valuable to address these issues rather than on-shore measurements, as no adjustments for snow redistribution on the ice would be required, leading to more accurate representation of snow ice/clear ice amounts. Currently, the parameterization of the albedo in CLIMo is based on measurements from High Arctic lake ice (Heron and Woo, 1994) where snow ice is less prevalent than clear ice (Woo and Heron, 1989). The use of an albedo decay model (Henneman and Stefan, 1999) or on-ice albedo measurements within CLIMo would be advantageous for capturing the seasonal changes to albedo—especially during the melt season when the higher albedo from snow ice (if present) would reflect more incoming radiation, slowing the absorption of solar radiation into the ice cover and reducing the melt rate.

Also, using a higher resolution setting on the camera imagery is possible and would facilitate the identification of melt onset as differentiating between snow free and melting/slush was difficult at times. This study has illustrated how these techniques can be beneficial not only for model validation but also for the monitoring of ice cover on lakes as very little remains of the lake ice observation network in Canada (Lenormand *et al.*, 2002). While other methods of monitoring ice cover are possible (e.g. volunteer monitoring programs such as IceWatch (Futter, 2003) or the use of remote sensing) a fully automated observing system can reduce discrepancies

introduced by multiple observers, provide continuous monitoring of the ice cover, and presents another viable option for rebuilding the lost network of ice monitoring stations in Canada.

ACKNOWLEDGEMENTS

The authors would like to thank David Fissel and Adam Bard of ASL Environmental Sciences Inc. for their assistance with the configuration and processing of the SWIP data. We would also like to acknowledge Arvids Sillis and all those who assisted in the collection of field data used in this study: Chris Derksen, Stephen Howell, Kevin Kang, Andrew Kasurak, Josh King, Merrin Macrae, Jason Oldham, Nicolas Svacina, Aiman Soliman, Peter Toose, as well as Ross Brown for providing the cloud cover data. Support for data collection from the Churchill Northern Studies Centre (CNSC) staff and Scientific Coordinator LeeAnn Fishback was appreciated. Financial support was provided through a Graduate Scholarship (L. Brown) and Discovery Grant (C. Duguay) from NSERC, and a CFI grant to C. Duguay and R. Kelly.

REFERENCES

- Adams WP, Roulet NT. 1984. Sampling of snow and ice on lakes. *Arctic* **37**(3): 270–275.
- Brown LC, Duguay CR. 2010. The response and role of ice cover in lake-climate interactions. *Progress in Physical Geography* **34**(5): 671–704.
- Duguay CR, Flato GM, Jeffries MO, Ménard P, Morris K, Rouse WR. 2003. Ice-cover variability on shallow lakes at high latitudes: model simulations and observations. *Hydrological Processes* **17**: 3465–3483.
- Flato GM, Brown RD. 1996. Variability and climate sensitivity of landfast Arctic sea ice. *Journal of Geophysical Research* **101**(C10): 25767–25777.
- Futter MN. 2003. Patterns and trends in southern Ontario lake ice phenology. *Environmental Monitoring and Assessment* **88**: 431–444.
- Henneman HE, Stefan HG. 1999. Albedo models for snow and ice on a freshwater lake. *Cold Regions Science and Technology* **29**: 31–48.
- Heron R, Woo MK. 1994. Decay of a High Arctic lake-ice cover: observations and modeling. *Journal of Glaciology* **40**: 283–292.
- Jasek M, Marko JR, Fissel D, Clarke M, Buermans J, Paslawski K. 2005. *Proceedings from the 13th Workshop on the Hydraulics of Ice-Covered Rivers*. (sponsored by CGU HS Committee on River Ice Processes and the Environment) Hanover, NH, 34 p.
- Jeffries MO, Morris K, Duguay CR. 2005. Lake ice growth and decay in central Alaska, USA: observations and computer simulations compared. *Annals of Glaciology* **40**: 1–5.
- Korhonen J. 2006. Long-term changes in lake ice cover in Finland. *Nordic Hydrology* **4–5**: 347–363.
- Launiainen J, Cheng B. 1998. Modelling of ice thermodynamics in natural water bodies. *Cold Regions Science and Technology* **27**: 153–178.
- Lenormand F, Duguay CR, Gauthier R. 2002. Development of a historical ice database for the study of climate change in Canada. *Hydrological Processes* **16**: 3707–3722.
- Liston GE, Hall DK. 1995. An energy-balance model of lake-ice evolution. *Journal of Glaciology* **10**: 373–382.
- Livingstone DM, Adrian R. 2009. Modeling the duration of intermittent ice cover on a lake for climate change studies. *Limnology and Oceanography* **54**: 1709–1722.
- Marko JR, Fissel DB. 2006. Marine Ice profiling: future directions. In *Proceedings from ICETECH 2006*, Banff, Canada, 6 p.
- Marko JR, Fissel DB, Jasek M. 2006. Recent developments in ice and water column profiling technology. In *Proceedings from the 18th IAHR Ice Symposium 2006*, Sapporo Japan, 8 p.
- Maykut GA, Untersteiner N. 1971. Some results from a time-dependant thermodynamic model of sea ice. *Journal of Geophysical Research* **76**: 1550–1575.
- Melling H, Johnston PH, Riedel DA. 1995. Measurements of the underside topography of sea ice by moored subsea sonar. *Journal of Atmospheric and Oceanic Technology* **12**: 589–602.
- Ménard P, Duguay CR, Flato GM, Rouse WR. 2002. Simulation of ice phenology on Great Slave Lake, Northwest Territories, Canada. *Hydrological Processes* **16**: 3691–3706.
- Ménard P, Duguay CR, Pivot FC, Flato GM, Rouse WR. 2003. Sensitivity of Great Slave Lake ice cover to climate variability and climatic change. In *Proceedings of the 16th International Symposium on Ice*. Dunedin, New Zealand, 2–6 December 2002, vol. 3: 57–63.
- Morris K, Jeffries M, Duguay C. 2005. Model simulation of the effects of climate variability and change on lake ice in central Alaska, USA. *Annals of Glaciology* **40**: 113–118.
- Palecki MA, Barry RG. 1986. Freeze-up and break-up of lakes as an index of temperature changes during the transition seasons: a case study for Finland. *Journal of Climate and Applied Climatology* **25**: 893–902.
- Rouse WR, Binyamin J, Blanker PD, Bussièrès N, Duguay CR, Oswald CJ, Schertzer WM, Spence C. 2008. The influence of lakes on the regional energy and water balance of the central Mackenzie. Chapter 18. In *Cold Region Atmospheric and Hydrologic Studies: The Mackenzie GEWEX Experience, vol. 1* Woo MK (ed). Springer-Verlag: Berlin; 309–325.
- Sturm M, Holmgren J, König M, Morris K. 1997. The thermal conductivity of seasonal snow. *Journal of Glaciology* **43**: 26–41.
- Vavrus SJ, Wynne RH, Foley JA. 1996. Measuring the sensitivity of southern Wisconsin lake ice to climate variations and lake depth using a numerical model. *Limnology and Oceanography* **41**: 822–831.
- Woo MK, Heron R. 1989. Freeze-up and break-up of ice cover on small arctic lakes. In *Northern Lakes and Rivers*, Mackay WC (ed). Boreal Institute for Northern Studies Occasional Publication 22: Edmonton; 56–62.